Epigenomic co-localization and co-evolution reveal a key role for 5hmC as a communication hub in the chromatin network of ESCs

Network approaches to decipher the epigenetic communication of embryonic stem cells

David Juan[1,*], Juliane Perner[2,*], Enrique Carrillo de Santa Pau[1,*], Simone Marsili[1,*], David Ochoa[3], Ho-Ryun Chung[4], Martin Vingron[2], Daniel Rico[1,$] and Alfonso Valencia[1,$]

[1]Structural Biology and BioComputing Programme, Spanish National Cancer Research Center - CNIO, Melchor Fernandez Almagro 3, 28029 Madrid, Spain.
[2]Computational Molecular Biology, Max Planck Institute for Molecular Genetics, Ihnestrasse 63-73, 14195 Berlin, Germany.
[3]European Bioinformatics Institute (EMBL-EBI), European Molecular Biology Laboratory, Wellcome Trust Genome Campus, Hinxton, Cambridge CB10 1SD, United Kingdom.
[4]Otto-Warburg-Laboratories Epigenomics, Max Planck Institute for Molecular Genetics, Ihnestrasse 63-73, 14195 Berlin, Germany.

*These authors contributed equally to this work.
[$]Corresponding authors: valencia@cnio.es, drico@cnio.es

Abstract

Epigenetic communication through histone and cytosine modifications is essential for gene regulation and in defining cell identity. Among the possible cytosine modifications, 5-hydroxymethylcytosine (5hmC) has been related with the pluripotent status of ESCs, although its precise functional role remains unclear. To fully understand the functional role of epigenetic modifications, it is necessary to analyze the whole chromatin network. Here, we propose a framework that is based on a communication model in which histone and cytosine modifications are considered epigenetic signals, while chromatin-associated proteins (CrPs) can act as emitters or receivers of these signals. We inferred the epigenetic communication network of mouse ESCs from genome-wide location data (77 different epigenomic features) combined with extensive manual annotation of epigenetic emitters and receivers based on the literature. Notably, 5hmC represents the most central hub of this network, connecting DNA demethylation to most of the nucleosome remodeling complexes and to several key transcription factors of pluripotency. An evolutionary analysis of the network revealed that most co-evolving CrP pairs are connected by 5hmC. Further analysis of the genomic regions marked with 5hmC and bound by specific interactors (ESRRB, LSD1, TET1 and OGT) shows that each interaction points to different aspects of chromatin remodeling, cell stemness, differentiation and metabolism. Taken together, our results highlight the essential role of cytosine modifications in the epigenetic communication of ESCs.

Introduction

Intracellular and intercellular communication between proteins and/or other elements in the cell is essential for homeostasis and to respond to stimuli. Communication may originate through multiple sources and it can be propagated through different compartments, including the cell membrane, the cytoplasm, the nuclear envelope or chromatin. Indeed, a cell's identity is defined by complex communication networks, involving chemical processes that ultimately modify the DNA, histones and other chromatin proteins ("epigenomic remodeling").

It has been proposed that multiple histone modifications confer stability, robustness and adaptability to the chromatin signaling network (Schreiber & Bernstein, 2002). In fact, it is now clear that the combination of different histone marks defines the epigenomic scaffolds that affect the binding and function of other epigenetic elements (e.g., different protein complexes). The increasing interest in characterizing the epigenomic network of many biological systems has led to an impressive accumulation of genome-wide experimental data from distinct cell types. This accumulation of experimental data has meant that the first chromatin signaling co-localization networks of histone marks and chromatin remodelers could be inferred in the fly (van Bemmel *et al*, 2013) and at promoters in human (Perner *et al*, 2014). However, we are still far from understanding the epigenomic "syntax" and how different chromatin components communicate with each other to control biological processes. In addition, a variety of cytosine modifications with possible regulatory roles have emerged as potentially important pieces of this 'chromatin puzzle', such as 5-methylcytosine (5mC), 5-hydroxymethylcytosine (5-hmC), 5-formylcytosine (5-fC) and 5-carboxylcytosine (5-caC: Ficz *et al*, 2011; Pastor *et al*, 2011; Williams *et al*, 2011; He *et al*, 2011; Ito *et al*, 2011; Raiber *et al*, 2012). However, the biological function and the role of these modifications in epigenetic signaling is not yet clear (Pfeifer *et al*, 2013; Liyanage *et al*, 2014; Moen *et al*, 2015). Moreover, we still do not understanding how these and the other elements involved in epigenomic communication shape the functional landscape of mammalian genomes.

It has been proposed that evolution can be used to discern the basis of meaningful communication in animals (Smith & Harper, 2003). The continuous adaptation of

78 living organisms to different scenarios requires a fine-tuning of molecular
79 communication. As a consequence, the conservation of communication pathways is
80 often challenged by ever-changing selection pressures. Recent research pointed to
81 protein co-evolution as a source of change in systems where the ability to interact
82 with the environment and adapt are essential for fitness (de Juan *et al*, 2013). In
83 addition, communication frequently occurs among mutualistic and symbiotic species,
84 as the evolution of communicative strategies requires co-adaptation between signal
85 production/emission and signal reception/interpretation (Smith & Harper, 2003; Scott-
86 Phillips, 2008). At a molecular level, long-standing protein co-evolution can be
87 reliably detected through directly correlated evolutionary histories. In fact, co-
88 evolutionary analysis has successfully identified molecular interactions at different
89 levels of detail (de Juan *et al*, 2013). As a consequence, protein co-evolution
90 signatures would be expected to clearly reflect essential communicative interactions
91 that have been frequently challenged by fluctuating evolutionary pressures.
92
93 Here, we establish a new framework to rationalize and study epigenomic
94 communication. This framework combines network-based analyses and an
95 evolutionary characterization of the interactions of chromatin components derived
96 from high-throughput data and literature mining. In particular, we followed a systems
97 biology approach to investigate the functional interdependence between chromatin
98 components in mouse embryonic stem cells (ESCs), whereby changes to their
99 epigenome control a very broad range of alternative cell differentiation options and
100 they are essential for lineage specification. We constructed the epigenetic signaling
101 network of ESCs as a combination of high-quality genomic co-localization networks
102 of 77 different epigenomic features: cytosine modifications, histone marks and
103 chromatin-related proteins (CrPs) extracted from a total of 139 ChIP-seq experiments.
104 We labeled histone marks and cytosine modifications as *signals* and we classified the
105 proteins that co-localize with them as their *emitters* (writers or erasers) or *receivers*
106 (readers) based on information in the literature **(Figure 1)**. To our knowledge the
107 resulting communication network is the most complete global model of epigenetic
108 signaling currently available and therefore, we propose it to be a valuable tool to
109 understand such processes in ESCs.
110

By analyzing this network, we found 5hmC to be a key node that mediates communication between different regions of the network. In addition, our co-evolutionary **analysis of this network identified 5hmC as a central node that connects most co-evolving CrPs**. Exploration of 5hmC-centered communication revealed that specific co-localization of 5hmC with the TET1, OGT, ESRRB and LSD1 produces alternative partner-specific activity, such as chromatin remodeling, cell stemness and differentiation, and energy metabolism. Thus, we propose that 5hmC acts as a central signal in ESCs for the self-regulation of epigenetic communication.

Results

Inference of the chromatin signaling network in mouse ESCs

We built an epigenetic signaling network in mESCs through a two-step process. First, we inferred the network connectivity based-on co-localization in the genome-wide distribution of chromatin components. In this analysis, we included 139 ChIP-Seq, MEDIP and GLIB assays for 77 epigenetic features (3 cytosine modifications, 13 histone marks and 61 CrPs: **Supplementary Table 1)**. Accordingly, we employed a method described recently (Perner *et al*, 2014) that reveals direct co-dependence between factors that cannot be "explained" by any other (indirect) factor observed. Thus, we detected only relevant interactions in different functional chromatin domains (see **Methods** for details).

Second, we annotated the direction of the interactions in the network (as shown in **Figure 1**), for which we relied on classifying a CrP as an emitter based-on previously reported experimental evidence of its specific ability to write or erase an epigenetic signal (either a histone mark or a cytosine modification, **Suppl. Table 2**). This evidence can be roughly summarized within two possible scenarios: (1) Protein A is a known *writer* or *eraser* of signal B; (2) Alterations to the genome-wide distribution of protein A (e.g., through its knock-out) affect the distribution of signal B in the genome. In the absence of any such evidence, proteins were defined as receivers of the interacting signal.

This epigenetic communication network (**Figure 2A**) recovered 236 connections between 68 nodes, the latter represented by cytosine modifications, histone marks or CrPs. The network contains 192 positive interactions (simultaneous interactions, 81.4%) and 44 negative (mutually exclusive interactions, 18.6%). A web interactive browser of the global co-localization network enables users to explore the interactions among these chromatin components in more detail (see http://dogcaesar.github.io/epistemnet).

Our approach detected 115 direct CrP-CrP interactions that are mostly due to protein complexes given that these components coincide at chromatin. These include complexes such as Polycomb (RYBP/CBX7/PHF19/SUZ12/EZH2), Cohesin (RAD21/SMC1/SMC3), Mediator (MED1/MED12/NIPBL), the nucleosome remodeling deacetylase MI2/NuRD complex (MI2B/LSD1/HDAC1/HDAC2) and CoREST/Rest (Rest/CoREST/RYBP: **Figure 2A**).

In order to understand the epigenetic interaction network and its activity as a communication system, we focused our analyses on directional interactions: *emitter-signal* and *signal-receiver* associations. Based on the experimental information extracted from the literature, we established “communication arrows" from “emitter-CrPs” to their signals and from the signals to their epigenetic "receiver-CrPs". In general, we could establish 124 (52.5%) directional interactions involving an epigenetic emitter and a signal (56 edges), or a receiver and a signal (68 edges), and as a consequence, we identified 8 emitter-CrPs, 17 receiver-CrPs and 18 CrP nodes that can act simultaneously as emitters and receivers of different signals.

The hubs of a network are highly connected nodes that facilitate the networking of multiple components. Directional edges allowed us to distinguish between two types of hubs: in-hubs (nodes with a large number of incoming arrows) and out-hubs (with a large number of outgoing arrows). Not surprisingly, the main in-hub was RNA polymerase II with S2 phosphorylation of the C-terminal (RNAPII_S2P). Indeed, 9 out of 16 signals in the network pointed to this form of RNAPII, which is involved in transcriptional elongation and splicing (**Suppl. Figure 1**). Here, the strong in-hub

175 nature of RNAPII_S2P in the network coincided with the many different signals that
176 independently contribute to transcription and expression in the genome.
177
178 By contrast, the two main out-hubs in the network revealed a different aspect of
179 epigenetic regulation. The main hubs that accumulated connections with receivers
180 were H3K79me2 (12) and 5hmC (10: **Figure 2B, Suppl. Figure 2**). H3K79me2 is
181 involved in transcription initiation and elongation, as well as promoter and enhancer
182 activity, suggesting that it is a key signal for different aspects of transcriptional
183 regulation. Interestingly, two groups of transcription factors (TFs) were connected to
184 H3K79me2: one composed of TCF3, OCT4, SOX2 and NANOG; and another that
185 contains CMYC, NMYC, STAT3, KLF4, TCFCP2L1 and E2F1. Conversely, 5hmC
186 is particularly interesting as it is thought to be a key element in different processes
187 even though its role in gene regulation remains controversial (Pfeifer *et al*, 2013;
188 Liyanage *et al*, 2014). Whereas initially related to gene activation (Song *et al*, 2011),
189 others claimed that 5hmC associates with weakly expressing poised promoters (Pastor
190 *et al*, 2011; Williams *et al*, 2011), while both roles were elsewhere claimed to be
191 possible depending on the context (Wu *et al*, 2011). In addition, 5hmC was shown to
192 play a major role in enhancer activation (Stroud *et al*, 2011; Szulwach *et al*, 2011) or
193 silencing (Choi *et al*, 2014). This apparent controversy could be explained by the role
194 of 5hmC as a central node of the communication network. Indeed, 5hmC was the
195 node that is traversed by the highest number of paths between nodes (**Suppl. Figures**
196 **3 and 4**), which implied that this node concentrates the information flow of the mESC
197 network.
198

199 **Co-evolution among chromatin components**

200 Cell stemness evolved very early in metazoan evolution and it is a critical
201 phenomenon that enhances the viability of multicellular animals (Hemmrich *et al*,
202 2012). Thus, it can be assumed that CrP-mediated communication in stem cells has
203 also been essential for metazoan evolution. As co-evolution consistently reflects
204 important functional interactions among conserved proteins (de Juan *et al*, 2013), we
205 studied the signatures of protein co-evolution within the context of the epigenetic
206 communication network in stem cells. We focused our analysis on the CrPs in the
207 network for which there is sufficient sequence and phylogenetic information in order

208 to perform a reliable analysis of co-evolution (de Juan *et al*, 2013). We extracted
209 evolutionary trees for 59 orthologous CrPs in our epigenetic communication network
210 and calculated their degree of co-evolution. To disentangle the direct and
211 uninformative indirect evolutionary correlations, we developed a method that
212 recovers protein evolutionary partners based on a maximum-entropy model of
213 pairwise interacting proteins (see Methods for specific details of the implementation).
214
215 Using this approach, we retrieved 34 significant co-evolutionary interactions among
216 54 CrPs (see **Supplementary table 3**). A total of 27 co-evolved relationships were
217 identified based on the direct functional protein-protein interactions evident in prior
218 experimental data: external sources, indirect evidence in the literature and/or from our
219 communication network (see **Supplementary Table 3**). These co-evolutionary
220 associations reflected the evolutionary relevance of different epigenetic
221 communication pathways that might be at play in essential, evolutionary maintained
222 cell types like ESCs.
223
224 We identified epigenetic signals that connect CrPs related by co-evolution (i.e.: those
225 connecting co-evolving pairs) and we considered the historically influential signals as
226 those that were best connected in a co-evolutionary filtered network. This co-
227 evolutionary filtered network was obtained by maintaining the pairs of CrPs that both
228 co-evolve and that are included in a protein/signal/protein triplet (see **Figure 3**). Co-
229 evolving CrP pairs are not evenly distributed in the epigenetic communication
230 network but rather, we found a statistically significant correspondence between
231 signal-mediated communication and co-evolution for H3K4me2, H3K4me3 and
232 5hmC (p-value < 0.05, see Methods). Of these, 5hmC mediates communication
233 between four different co-evolving pairs and seven different CrPs (**Figure 3**), clearly
234 standing out as the epigenetic signal connecting more co-evolving CrPs. Notably, the
235 three positively co-occurring emitters of 5hmC (TET1, OGT and LSD1) co-evolved
236 with three different receivers (MBD2, TAF1 and SIN3A). Thus, from the
237 combination of the 5hmC interactors (see **Fig. 2C**), three specific
238 emitter/signal/receiver triplets with coordinated evolution were identified: LSD1-
239 5hmC-SIN3A, TET1-5hmC-MBD2 and OGT-5hmC-TAF1. In other words, co-
240 evolutionary signals reflected very important interactions due to the multiple

connections that are possible in the network. In addition, we detected co-evolution between the 5fC-emitter BRG1 and the 5fC-receiver NIPBL.

The case of MBD2 and TET1 is particularly interesting given the biological activities of these proteins. One of the key functions of TET1 is the oxidation of 5mC, while MBD2 is a methyl-binding domain protein (MBD) that shows higher binding affinity to 5mC than to 5hmC (Baubec *et al*, 2013). In addition, MBDs are thought to modulate 5hmC levels, inhibiting TET1 by their binding to 5mC (Hashimoto *et al*, 2012). The co-evolution of MBD2 and TET1 suggests certain dependence between the mechanisms that maintain 5mC and 5hmC at different epigenomic locations in ESCs.

The well-known TET1 interactors OGT and SIN3A each co-evolved with a different CrP: TAF1 and LSD1, respectively. OGT co-occurs with 5hmC while TAF1 binding is significantly enriched in 5hmC depleted regions. Similarly, LSD1 positively interacts with 5hmC while its co-evolving partner SIN3A was found in a pattern that is mutually exclusive to 5hmC. As in the case of TET1 and MBD2, these results suggest the remarkable influence of 5hmC on the differential binding of CrPs to distinct genomic regions in the ESC epigenome during metazoan evolution.

Accordingly, these results confirmed our working hypothesis that chromatin proteins interconnected via epigenetic signals have evolved in a concerted manner. Interestingly, our results also suggest that 5hmC is a communication hub as it connects processes that have been coordinated during metazoan evolution.

Functional modularization of the network reveals protein complexes and star-shaped structures

Having shown that 5hmC and H3K79me2 are the most influential signals in the ESC epigenetic communication network, and that 5hmC mediates the communication between CrPs that have co-evolved in Metazoa, recent research has shown that the genomic localization of certain combinations of core epigenetic features allows different chromatin states associated with functional processes to be reliably identified (Filion *et al*, 2010; Ernst & Kellis, 2010). Here, we examined how the

positive interactions in the network are distributed in relation to these different functional contexts. In particular, we focused on the modules of co-localizing chromatin components with similar peak frequencies that were associated with the diverse chromatin states in ESCs (see Methods and **Supplementary Fig. 5**).

We found 15 groups of interactions that yielded sub-networks associated with distinctive functional chromatin profiles (**Figure 4**). These **chrom**atin context-specific **net**works (*chromnets*) were made up of CrPs and epigenetic signals that tended to co-exist in the different chromatin states at a similar frequency in ESCs. We found that most chromnets could be classified into two groups: protein complexes and communication chromnets. Specific examples of protein complexes chromnets were Polycomb (CBX7/PHF19/SUZ12/EZH2) in chromnet-5, Cohesin (RAD21/SMC1/SMC3) in chromnet-10 or Mediator (MED1/MED12/NIPBL) in chromnet-11 (**Figure 4A and Supp. Figs 6-20**). These chromnets had high clustering coefficients and a high proportion of CrP-CrP interactions, and their frequency in different chromatin states was coherent with their known function. For example, chromnet-5 (Polycomb) was strongly enriched in the two chromatin states enriched in H3K27me3 (**Supp. Figure 10**).

We also noted the presence of star-like chromnets with very low clustering coefficients. These star-like chromnets are mostly generated by emitter/signal and signal/receiver interactions, suggesting that these are communication modules that connect different protein complexes. For example, chromnet-3 contains two central connectors (5fC and RYBP) connecting Polycomb, Mediator and TET1-SIN3A complexes, and this chromnet is enriched in active transcription states and regulatory elements (**Suppl. Figure 8**).

Interestingly, chromnet-2 was a star-like module centered on 5hmC (the most central hub in the network) and it contained all its positively co-localizing interactors: LSD1, RYBP, ESRRB, KDM2A, TET1, OGT, G9A, and MBD2T (**Figure 4B**). In addition, 5hmC indirectly connects to H3K4me1 via TET1, and with 5mC via MBD2T. This chromnet was clearly enriched in regulatory elements.

307 In summary, we have decomposed the communication network into communication
308 chromnets, functional modules of interactions with similar frequencies in the different
309 chromatin contexts. The components, structure and genomic distribution of these
310 chromnets provided information about their functional role. In particular, we detected
311 several star-like chromnets that are important to distribute epigenetic information to
312 different regions of the communication network. The wide range of functional
313 chromatin states that were enriched in these chromnets further supports their potential
314 role in mediating communication between distinct processes.
315

316 **Independent co-localization of 5hmC with ESRRB, LSD1, OGT and TET1 was**
317 **associated with different biological activities**

318 Having identified 5hmC as an important communication signal in extant mouse ESCs
319 and during metazoan evolution, we also found that the eight positive interactions (co-
320 existence) between 5hmC and CrPs are part of a star-like chromnet with similar
321 enrichment associated with chromatin states. We further characterized the genomic
322 regions where 5hmC co-localized independently with the stemness factor ESRRB and
323 with the three independent emitters of 5hmC, LSD1, OGT and TET1, which were
324 also identified in our co-evolutionary analysis (see above).
325

326 Remarkably, we found 6,307 genomic regions where 5hmC co-localized with its
327 receiver ESRRB in the absence of TET1, and with the rest of its interactors (**Figure**
328 **5A**). ESRRB is a transcription factor that is essential for the maintenance of ESCs
329 (Papp & Plath, 2012; Zwaka, 2012), yet to our knowledge the binding of ESRRB to
330 DNA has not been previously associated with the presence of 5hmC. However, the
331 ESRRB gene locus is known to be strongly enriched in 5hmC in ESCs (Doege *et al*,
332 2012), suggesting that 5hmC and ESRRB form a regulatory loop. **Gene ontology**
333 **analysis** carried out with the genes closest to these specific regions (McLean *et al*,
334 2010) identified stem cell maintenance, MAPK and Notch cell signaling cascades as
335 the most enriched functions **(Figure 5E)**, highlighting the importance of ESRRB for
336 stemness maintenance. Surprisingly, the expression of the ESRRB gene is not ESC-
337 specific but rather it is expressed ubiquitously in most differentiated cell types
338 (Zwaka, 2012). Thus, its specific role in stemness probably requires ESC-specific
339 interactions with other components of the communication network and our results

340 suggested that 5hmC might be the key signal connecting ESRRB function with
341 stemness.
342
343 LSD1 is a H3K4- and H3K9-demethylase that can act as either a transcriptional co-
344 activator or co-repressor (Wang *et al*, 2007). To our knowledge, this was the first time
345 5hmC and LSD1 were found to coincide in the epigenome of ESCs (**Figure 5B**).
346 Interestingly, it is well known that there is a functional co-dependence between
347 histone demethylation and DNA methylation (Vaissière *et al*, 2008; Ikegami *et al*,
348 2009). Indeed, we consider LSD1 is an emitter of 5hmC because there is a global loss
349 of DNA methylation in the LSD1 knockout (Wang *et al*, 2009, 1). Remarkably, we
350 found that the 9,714 5hmC-**LSD1 specific** regions are significantly enriched with
351 specific terms associated with histone acetylation and DNA modification (**Figure**
352 **5E**), strengthening the dependent relationship between histone and DNA
353 modifications. Indeed, LSD1 not only functions as a histone demethylase by itself but
354 also, in association with 5hmC it can regulate the expression of proteins that modify
355 both histone acetylation and DNA methylation. These results suggest the presence of
356 a second regulatory loop involving 5hmC.
357
358 TET1 and OGT are two of the best known emitters of 5hmC (**Figure 5C-D**), with
359 TET1 a DNA demethylase that catalyzes the conversion of 5mC to 5hmC and OGT a
360 regulator of TET1 (Vella *et al*, 2013; Balasubramani & Rao, 2013). In fact, the role of
361 OGT in DNA demethylation was associated to its co-localization with TET1.
362 However, OGT is a N-acetylglucosaminyltransferase that can also bind to different
363 TFs independently of TET1 (Bond & Hanover, 2015). Notably, we observed different
364 functional enrichment of the 5hmC-TET1 and 5hmC-OGT regions (**Figure 5E**).
365 While the 27,721 5hmC-TET1 regions were enriched in stem cell maintenance and
366 morphogenesis, highlighting the role of both 5hmC and TET1 in stemness, the 1,017
367 5hmC-OGT regions were related with the metabolism of glycerophospholipids and
368 carbohydrates. Interestingly, OGT is known to bind phosphatidylinositol-3,4,5-
369 trisphosphate, regulating insulin responses and gluconeogenesis through glycosylation
370 of different proteins (Yang *et al*, 2008). Our results suggest that the alternative role of
371 OGT in gene regulation is also associated to 5hmC (but not to TET1). As the presence
372 of 5hmC requires the action of TET1, our results suggest that OGT might remain in
373 certain locations after TET1 removal, probably associated to the presence of specific

TFs in order to regulate the metabolism of glycerophospholipids and carbohydrates. In this scenario, OGT would act as an emitter regulating 5hmC production and as a receiver by acting with other proteins in the presence of 5hmC to regulate gene expression.

In summary, the analysis of specific genomic regions revealed that different processes and functions could be regulated and may be interconnected via 5hmC interactions with other proteins. These processes include functions as relevant as epigenetic self-regulation, cell signaling, maintaining stemness, morphogenesis and metabolism.

Discussion

ESCs constitute an ideal model to explore the epigenomic communication that directly influences the phenotype of cells. Cytosine modifications, certain histone marks and CrPs contribute to the plasticity required for the induction and maintenance of pluripotency. Thus, the abundant epigenomic data from mouse ESCs has enabled us to investigate how the different chromatin components communicate with each other within a complex network. Using high-throughput genome-wide data and information from the literature, we reconstructed the epigenetic communication network of ESCs. In addition to the rigorously established co-incidence and mutual exclusion, we also annotated the directions of the CrP interactions mediated by epigenetic signals (cytosine modifications and histone marks) based on information extracted manually from the literature. This information allows CrPs to be classified as emitters or receivers of these more basic epigenetic signals.

Our results provide a framework for future studies of the chromatin network in ESCs and other cell types, and we highlight the importance of using information taken from the literature. This biological knowledge allowed us to understand the network of co-localization patterns from high-throughput data, permitting us to obtain the first global picture of the information flow that could take place in the ESC epigenome. For example, we identified the hubs that receive more independent signals - in-hubs - and those that emit signals to a larger number of receivers - out-hubs. Not surprisingly, active RNA polymerase II was identified as the main in-hub of the

network, which shows that our approach is able to recover biologically meaningful, data, as many components of the network regulate transcription.

More surprisingly, our analysis revealed that 5hmC is the main out-hub and the most central node in this network. 5hmC interacts with a total of sixteen CrPs: five emitters of 5hmC and eleven receivers. Of these sixteen interactions, half are positive (co-occurrence) and half are negative (mutual exclusion). The large number of CrPs that preferentially bind to chromatin in the presence or absence of 5hmC indicates that this cytosine modification is an influential signal for chromatin communication in ESCs.

The elements that drive epigenetic communication constitute an intricate and dynamic network that produces responses that range from stable programs defining cell-identity to fast cellular responses. In this context, the fine-tuning of epigenetic communication pathways is likely to have been a key aspect in the evolution of multicellular organisms, such as metazoans. Co-evolutionary analyses highlight the conservation and co-ordinated changes in interactions, and this is a particularly adequate approach to reveal strong functional links in the context of complex and dynamic protein interactions. Co-evolution can occur between proteins that interact directly or that participate in the same communication processes – for example, via chromatin interactions mediated by histone marks or cytosine modifications.

Remarkably, the majority of the co-evolutionary associations related to epigenetic communication are triplets formed by an emitter, a signal and a receiver. Unexpectedly, four different co-evolutionary associations were found between proteins interacting with 5hmC: SIN3A with LSD1, TET1 with MBD2, MBD2 with MLL2, and OGT with TAF1. Strikingly, all three co-occurring 5hmC emitters (TET1, OGT and LSD1) co-evolve with three different 5hmC receivers, forming different emitter-5hmC-receiver triplets. Interestingly, these associations do not reflect direct physical interactions of the protein pairs but rather, complementary roles in the control of cytosine modifications and gene regulation. Thus, we speculate that the balance between 5mC, 5hmC and other cytosine modifications has been very important in fine-tuning epigenomic communication during the evolution of metazoans.

Identifying modules in networks helps better understand their distinct components (Mitra *et al*, 2013). Here, we followed a simple approach to identify functional sub-networks of chromatin communication, or chromnets, clustering positive interactions in function of their relative frequency in different chromatin states. This analysis revealed the functional structure of the communication network and we were able to automatically recover known protein-complexes, such as Polycomb and Mediator. By contrast, we found that 5hmC and 5fC establish two different star-shaped chromnets, suggesting that they might be involved in communication between distinct epigenetic components and processes in distinct locations of the ESC epigenome.

While further experiments will be needed to reveal the functional roles of the different independent interactions of 5hmC, our results generate some interesting hypotheses about the possible independent functions played by 5hmC in ESCs. We propose that the stem-specific role of ESRRB in ESCs could be linked to its co-occurrence with 5hmC, as this cytosine modification is less common in most differentiated cell types (Zwaka, 2012). Our results also show that LSD1-5hmC might be specifically involved in the regulation of histone modifications and DNA methylation, while the TET1-5hmC interaction is associated with stem cell maintenance and morphology. Furthermore, our data suggest a TET1-independent interaction between 5hmC and OGT might participate in the regulation of energy metabolism, and an interaction between 5hmC and LSD1 regulates histones and DNA methylation.

The combination of genome-wide location data, prior knowledge from the literature and protein co-evolution highlights conserved functional relationships between 5hmC-interacting CrPs that have been dynamically coordinated during evolution. Based on our co-evolution analysis, we hypothesize that the different cytosine modifications in different regions of the genome might have been important during metazoan evolution. Our results suggest that the interaction of 5hmC with specific emitters is involved in regulating different specific and critical functions.

In conclusion, network architecture conveys relevant contextual information that cannot be easily obtained from analyses that focus on only a few epigenetic features.

472 The computational framework introduced here represents the basis to explore this vast
473 space and it provides the first integrated picture of the different elements involved in
474 epigenetic regulation. Accordingly, this analysis enables us to attain an integrated
475 vision of epigenetic communication in ESCs that highlighted the relevance of 5hmC
476 as a central signal. Notwithstanding, we are still at the early stages of exploring the
477 epigenetic network. Thus, the future inclusion of experimental data regarding
478 genome-wide localization profiles for many additional proteins, as well as that related
479 to other states of cell differentiation, will make it possible to draw-up a more
480 complete picture and to define the dynamics of the epigenetic network in different cell
481 lineages.
482
483

484 Materials and Methods

485 **ChIP-Seq, MeDIP and GLIB data processing**

486 We downloaded sra files from 139 Chromatin Immunoprecipitation Sequencing
487 (ChIP-Seq), Methylated DNA immunoprecipitation (MeDIP) and GLIB
488 (glucosylation, periodate oxidation and biotinylation) experiments described in
489 Supplementary Table 1. This collection includes 3 types of cytosine modifications
490 (5mC, 5hmC and 5fC), 13 histone marks (H2Aub1, H2AZ, H3K4me1, H3K4me2,
491 H3K4me3, H3K9ac, H3K9me3, H3K27ac, H3K27me3, H3K36me2, H3K36me3,
492 H3K79me2, H4K20me3) and 61 different Chromatin related Proteins (CrPs).
493 CrPs include structural proteins, elements of the machinery involved in cytosine
494 and histone modification, transcription factors (TFs, such as the stemness-
495 related TFs NANOG, OCT4 and SOX2), and four different post-translational
496 modifications of RNA polymerase II (RNAPolII: S2P, S5P, S7P and 8WG16 -
497 unmodified) with binding data available for ESCs. The MeDIP data for 5mC and
498 the GLIB data for 5hmC were taken from Pastor et al (Pastor *et al*, 2011) as it has
499 been previously shown that these datasets are less biased to antibody affinity in
500 regions with repeats than other methods (Matarese *et al*, 2011). The sra files were
501 transformed into fastq files with the sra-toolkit (v2.1.12) and aligned to the reference
502 mm9/NCBI37 genome with bwa v0.5.9-r16 (Li & Durbin, 2009) allowing 0-1
503 mismatches. Unique reads were converted to BED format.

504

505 **Genome segmentation**

506 The input information used to segment the genome into different chromatin states was
507 that derived from the 3 cytosine modifications, the 13 histone marks and the insulator
508 protein CTCF - which has been previously shown to define a particular chromatin
509 state *per se* (Ernst & Kellis, 2010). A multivariate Hidden Markov Model (HMM)
510 was employed that uses two types of information: the frequency with which different
511 combinations of chromatin marks are found with each other, and the frequency with
512 which different chromatin states are spatially related in the genome. To apply this
513 method we used the ChromHmm software (Ernst & Kellis, 2012: v1.03). The input
514 data to generate the model were the ChIP-Seq, MeDIP and GLIB bed files containing
515 the genomic coordinates and strand orientation of the mapped sequences (see above).
516 First, the genome was divided in 200 bp non-overlapping segments which were
517 independently assigned a value of 1 or 0 in function of the presence or absence of
518 histone marks, respectively, based on the count of the tags mapping to the segment
519 and on a Poisson background model (Ernst & Kellis, 2012) using a threshold of 10^{-4}.
520 After establishing a binary distribution for each mark, we trained the HMM model
521 using a fixed number of randomly-initialized hidden states that varied from 20 to 33
522 states. We focused on a 20-state model that provided sufficient resolution to resolve
523 biologically meaningful chromatin patterns according to previous selection strategies
524 (Ernst & Kellis, 2012; Kharchenko *et al*, 2011 - see Suppl. Figure 21). We used this
525 model to compute the probability that each location is in a given chromatin state and
526 we then assigned each 200 bp segment to its most likely state (see **Suppl. Tables 4**
527 **and 5**). Only, intervals with a probability higher than 0.95 were considered for further
528 analysis.

529 We identified states related with enhancer (states 1-3), transcription elongation
530 (states 4-5), heterochromatin (6-10), enhancers (11-14), promoter activation
531 (15-17), Polycomb (18-19) and the CTCF insulator (20), that are consistent with
532 prior knowledge regarding the function of these features (**Suppl. Figures 21, 22**
533 and **Suppl. Table 6**).

534

535 **Segment enrichment**

536 The proportion of overlap for each state and annotation in the genome was computed
537 with ChromHmm software on the selected segments (see above). The genomic
538 annotations, CpG islands, repeats and laminB1 annotations were downloaded from
539 the UCSC Genome Browser, and DNAseI and RNAseq were obtained from
540 ENCODE E14 cell line (see **Suppl. Table 1**). The processed CAGE data (Fort *et al*,
541 2014) and ChIA-PET data (Zhang *et al*, 2013) for ESCs were downloaded from the
542 supplementary material of the original papers (see **Suppl. Table 1**). The enrichment
543 of the annotations and CrPs can be consulted in **Suppl. Tables 7 and 8**.
544
545 **Read counts and pre-processing for the co-location network inference**
546 We used the ChromHMM segments with a probability higher than 0.95 as samples for
547 the network inference. We filtered all bins for each state that were unexpectedly large
548 (the upper 1% for each state) because they might produce outliers in the data and it is
549 hard to justify where the signal occurs within the region (**Suppl. Figure 23**). We
550 counted the overlapping ChIP-Seq reads for the resulting segments using Rsamtools,
551 although some of the ChIP-experiments had to be excluded from the network
552 inference due to the low number of reads per bin, or the low number of bins with
553 signal or study dependent artifacts, including: CTCF_GSE11431,
554 NANOG_GSE11431, LAMIN1B and H3K27me3_GSE36114, SMAD1_GSE11431,
555 MBD1A_GSE39610, MBD1B_GSE39610, MBD2A_GSE39610,
556 MBD3A_GSE39610, MBD4_GSE39610, and MECP2_GSE39610 (as MBD2A was
557 not used, the MBD2 co-localization data corresponds to MBD2T). Using hierarchical
558 clustering with 1-cor(x,y) as a distance measure, we find that most replicates or
559 functionally related samples fall into the same branch (**Suppl. Figures 24 and 25**).
560 Next, the replicates were merged by adding up the read counts in each segment. The
561 resulting 71 samples were normalized against the corresponding input using the same
562 method described in (Perner *et al*, 2014). In short, we estimated the median fold-
563 change of the sample over the input and used this median to shrink the change in each
564 segment towards 1. Finally, the data was log-transformed adding a pseudocount of 1.
565
566 **Co-location network inference**
567 To detect specific interactions between the components based on their co-localization
568 it is necessary to eliminate indirect/transitive effects, i.e.: co-localization that might be

569 introduced by other factors. To this end, we applied the method described in (Perner
570 *et al*, 2014) that aims to unravel the interactions between factors that cannot be
571 "explained" by the other observed factors and thus, this is a more specific approach
572 than an analysis of simple pair-wise correlations.
573 We inferred an interaction network for each chromHMM state. Briefly, for each state
574 the samples were scaled to have a mean of 0 and a standard deviation of 1. An Elastic
575 Net was trained in a 10-fold Cross-validation to predict the HM/CTCF/DNA
576 methylation of the CrPs or to predict each CrP from all other CrPs. Furthermore, the
577 sparse partial correlation network (SPCN) was obtained using all the samples
578 available. To visualize the final networks, we selected the interactions between
579 Histone marks/cytosine modifications and CrPs that obtained a high coefficient (w >=
580 2*sd(all_w)) in the Elastic Net prediction and that have a non-zero partial correlation
581 coefficient in the SPCN. All median coefficients of the Elastic Net, as well as the R^2-
582 values of the prediction over the 10-fold CV per state, are given in **Suppl. Tables 9**
583 **and 10**. All partial correlation coefficients of the SPCN per state are given in
584 **Suppl. Table 11**.
585 The global network with the information of all the states (**Figure 2A**)
586 summarizes all the direct interactions between cytosine modifications, histone
587 marks and CrPs. The global network, as well as the chromnets, can be explored
588 using EpiStemNet, an interactive viewer of the "co-location" network
589 (http://dogcaesar.github.io/epistemnet).
590
591 **Co-evolution-based analysis**
592 We retrieved 46,041 protein trees of sequences at the metazoan level from eggnog
593 v4.0 (Powell *et al*, 2014), including over a million protein sequences. These trees
594 include proteins from NS = 88 metazoan species that are either orthologs or paralogs
595 that were duplicated after the metazoan speciation split. Based on these trees, we
596 extracted only-unique-orthologous protein trees for each mouse protein by inferring
597 speciation and duplication nodes using a species-tree reconciliation approach
598 (Nenadic & Greenacre, 2007) and a previously developed pipeline to deal with tree
599 inconsistencies (Juan *et al*, 2013). When more than one ortholog was detected for a
600 mouse protein in a species, the one selected was that extracted from the tree with the
601 shortest overall evolutionary distance. As a result, we obtained 13,579 only-unique-

orthologous protein trees. From these, we extracted those that included the mouse proteins for which ChIP-seq data was analyzed in this study, before performing the main analysis on NP = 58 different protein trees that include mouse CrPs. The whole population of trees was kept to perform a randomization test in order to assign empirical statistical significance to our results.

We encoded each protein tree as a vector containing the NS(NS – 1)/2 distances between all the pairs of species in the analysis, and we formed a NS(NS – 1) X NP distance matrix containing these vectors as columns. Each row in this matrix represents a different instance of the distances in the set of proteins for a different pair of species. For each row of the matrix, the distances were ranked and binned into five equally populated intervals {ss,s,m,l,ll} according to the four quintiles of the distribution: ss (very short distances), s (short distances), m (around the median), l (large distances), ll (very large distances). An additional state, NA, was used for any missing values in the distance matrix. Denoting two generic proteins as p,q and two generic intervals as a,b, the single and pair frequencies $f_p(a)$ for protein p in bin a and $f_{p,q}(a,b)$ for the pair p,q in bins a,b were computed as averages over the pairs of species for p,q in {1,2,...,NP} and a,b in {ss,s,m,l,ll,NA}.

The maximum-entropy distribution in the space of the species-species distance bins {d} for fixed single and pair protein frequencies is given by:

$$P(\{d\}) = Z^{-1} \exp[\, \Sigma_p\, h(d_p) + \Sigma_{p,q}\, J_{p,q}(d_p,d_q)\,]$$

where Z is the partition function and the parameters h_p and $J_{p,q}$ have to be adjusted in order to match the empirical frequencies f_p and $f_{p,q}$. The parameters $J_{p,q}$ are of special interest here since they regulate the interactions between proteins in the model. For example, a strongly positive parameter $J_{p,q}(ss,ss)$ can be interpreted as the direct symmetrical interaction between the two proteins p and q, favoring the co-occurrence of short distances in the respective trees. The model parameters were determined by maximizing an l_2-regularized version of the (log) pseudo-likelihood (Besag, 1977) of the data:

$$\{\theta_k^*\} = \mathrm{argmax}_\theta[\, l_{pseudo}(\{\theta_k\}) - \lambda\, \Sigma_k\, \theta_k^2\,]$$

where θ_k denotes a generic parameter of the model and $\lambda = 0.01$.

633 We determined a co-evolutionary coupling $C_{p,q}$ for each pair of proteins p,q from the
634 related set of couplings between bins, represented by the matrix $J_{p,q}(a,b)$ with a,b in
635 {ss,s,m,l,ll}. Bin couplings involving missing values in the original set of distances
636 (NA state) were not included in the definition of $C_{p,q.}$ Following an established
637 protocol for contact prediction in protein structural analysis (Ekeberg *et al*, 2013), we
638 double-centered the matrix $J_{p,q}$ and computed the Frobenius norm $F_{p,q} = [\ \Sigma_{a,b\ =\ ss,s,m,l,ll}$
639 $J_{p,q}(a,b)^2\ ]^{1/2}$.
640 Finally, we applied an average product correction (Dunn *et al*, 2008) obtaining the co-
641 evolutionary coupling between proteins p and q, $C_{p,q} = F_{p,q} - F_pF_q/F$.
642
643 In order to assign statistical significance to our co-evolutionary couplings, we
644 randomly selected 10,000 groups of mouse proteins from the same size as our set of
645 chromatin modifiers. We ran the pipeline described above for every random set and
646 retrieved the corresponding matrix of co-evolutionary couplings. P-values were
647 assigned based on the random distribution obtained and associations supported by p
648 values < 0.05 were further considered. The matrix of co-evolutionary couplings and
649 corresponding p values are included in **Suppl. Table 3**.
650
651 This large-scale approach allows us to detect significant connections between
652 functional and structural modules by dissecting direct protein-protein co-evolutionary
653 relationships from the large "hairball" of indirect interactions (Weigt *et al*, 2009; de
654 Juan *et al*, 2013).
655
656 **Identification of epigenetic signals with a statistically significant co-evolutionary**
657 **effect**
658 For each epigenetic signal (histone mark/cytosine modification), we identified all the
659 pairs of CrPs that satisfy the following two conditions: 1) the proteins in the pair are
660 co-evolutionary coupled (see above); and 2) each of the proteins in the pair directly
661 interacts with the epigenetic signal. We then used the number of unique CrPs in the
662 resulting set of pairs (Co-evolutionary Filtered Centrality, CFC) as a measure of the
663 influence of the signal on co-evolution between the CrPs in the epigenetic signaling
664 network. The analysis resulted in 7 signals with a CFC greater than zero: H3K4me1
665 (CFC=2), H3K4me2 (4), H3K4me3 (5), H3K9ac (4), H3K27ac (2), 5fC (2), 5hmC

666 (9). 5hmC is clearly the signal with the strongest effect on co-evolution, with a
667 CFC=9 almost double that of the second ranking signal (H3K4me3).
668 The statistically significance of each CFC was evaluated by computing a p-value that
669 corresponded to the probability of obtaining a CFC greater or equal to that observed
670 in a network model with randomly-generated edges among the CrPs in the co-
671 evolutionary analysis. This procedure identified three signals with a significant CFC
672 (p-value < 0.05): 5hmC (p-value approx 0.04), H3K4me2 (0.01), H3K4me3 (0.02).
673

674 **Functional Modularization of the Co-localization Network**

675 The co-localization network was decomposed into local networks of positive
676 interactions. First, we calculated the frequency of each positive interaction using
677 ChromHMM peaks, considering that an interaction is present if both interactors are
678 'present' in the same 200 bp genomic window. We calculated this frequency for each
679 of the 20 chromatin states, such that we have a vector of 20 frequencies for each
680 positive interaction. In order to reduce state-specific biases, the frequencies of the
681 interactions were standardized separately for every state. These vectors were clustered
682 by hierarchical clustering (Pearson correlation, average linkage) and the largest
683 statistically supported clusters (p-value < 0.05, n=10,000) according to Pvclust
684 (Suzuki & Shimodaira, 2006) were defined as chromnets (see **Supp. Figure 5**).
685

686 **Gene Ontology enrichment analysis**

687 Gene Ontology enrichment analyses were carried out with GREAT v3.0.0 (McLean *et*
688 *al*, 2010). We used the independent segments of 5hmC co-localization with its
689 emitters and receivers as the input to predict biological functions of the associations
690 analyzing the closest genes. The genomic regions were associated to genes with a
691 minimum distance of 5Kb upstream and 1Kb downstream, with the whole genome as
692 the background. The False Discovery Rate (FDR) considered was 0.05 (see
693 Supplementary Table 12).
694

695 **URLs**

696 UCSC Trackhub with chromatin states, cytosine modifications, histone marks and
697 CrPs
698 http://genome.ucsc.edu/cgi-
699 bin/hgTracks?db=mm9&hubUrl=http://ubio.bioinfo.cnio.es/data/mESC_CNIO/mESC_CNIO_hub2/hub.txt

EpiStemNet: chromatin state specific co-location networks in ESCs

http://dogcaesar.github.io/epistemnet

Acknowledgements

Author contributions

Conflict of interest

Funding

References

Balasubramani A & Rao A (2013) O-GlcNAcylation and 5-Methylcytosine Oxidation: An Unexpected Association between OGT and TETs. *Mol. Cell* **49:** 618–619

Baubec T, Ivánek R, Lienert F & Schübeler D (2013) Methylation-Dependent and -Independent Genomic Targeting Principles of the MBD Protein Family. *Cell* **153:** 480–492

Van Bemmel JG, Filion GJ, Rosado A, Talhout W, de Haas M, van Welsem T, van Leeuwen F & van Steensel B (2013) A network model of the molecular organization of chromatin in Drosophila. *Mol. Cell* **49:** 759–771

Besag J (1977) EFFICIENCY OF PSEUDO-LIKELIHOOD ESTIMATION FOR SIMPLE GAUSSIAN FIELDS. *BIOMETRIKA* **64:** 616–618

Bond MR & Hanover JA (2015) A little sugar goes a long way: the cell biology of O-GlcNAc. *J. Cell Biol.* **208:** 869–880

Choi I, Kim R, Lim H-W, Kaestner KH & Won K-J (2014) 5-hydroxymethylcytosine represses the activity of enhancers in embryonic stem cells: a new epigenetic signature for gene regulation. *BMC Genomics* **15:** 670

Doege CA, Inoue K, Yamashita T, Rhee DB, Travis S, Fujita R, Guarnieri P, Bhagat

731 G, Vanti WB, Shih A, Levine RL, Nik S, Chen EI & Abeliovich A (2012) Early-
732 stage epigenetic modification during somatic cell reprogramming by Parp1
733 and Tet2. *Nature* **488:** 652–655
734 Dunn SD, Wahl LM & Gloor GB (2008) Mutual information without the influence
735 of phylogeny or entropy dramatically improves residue contact prediction.
736 *BIOINFORMATICS* **24:** 333–340
737 Ekeberg M, Lovkvist C, Lan Y, Weigt M & Aurell E (2013) Improved contact
738 prediction in proteins: Using pseudolikelihoods to infer Potts models. *Phys.*
739 *Rev. E* **87:** 012707
740 Ernst J & Kellis M (2010) Discovery and characterization of chromatin states for
741 systematic annotation of the human genome. *Nat. Biotechnol.* **28:** 817–825
742 Ernst J & Kellis M (2012) ChromHMM: automating chromatin-state discovery
743 and characterization. *Nat. Methods* **9:** 215–216
744 Ficz G, Branco MR, Seisenberger S, Santos F, Krueger F, Hore TA, Marques CJ,
745 Andrews S & Reik W (2011) Dynamic regulation of 5-hydroxymethylcytosine
746 in mouse ES cells and during differentiation. *Nature* **473:** 398–402
747 Filion GJ, van Bemmel JG, Braunschweig U, Talhout W, Kind J, Ward LD, Brugman
748 W, de Castro IJ, Kerkhoven RM, Bussemaker HJ & van Steensel B (2010)
749 Systematic protein location mapping reveals five principal chromatin types
750 in Drosophila cells. *Cell* **143:** 212–224
751 Fort A, Hashimoto K, Yamada D, Salimullah M, Keya CA, Saxena A, Bonetti A,
752 Voineagu I, Bertin N, Kratz A, Noro Y, Wong C-H, de Hoon M, Andersson R,
753 Sandelin A, Suzuki H, Wei C-L, Koseki H, Hasegawa Y, Forrest ARR, et al
754 (2014) Deep transcriptome profiling of mammalian stem cells supports a
755 regulatory role for retrotransposons in pluripotency maintenance. *Nat.*
756 *Genet.* **46:** 558–566
757 Hashimoto H, Liu Y, Upadhyay AK, Chang Y, Howerton SB, Vertino PM, Zhang X &
758 Cheng X (2012) Recognition and potential mechanisms for replication and
759 erasure of cytosine hydroxymethylation. *Nucleic Acids Res.* **40:** 4841–4849
760 Hemmrich G, Khalturin K, Boehm A-M, Puchert M, Anton-Erxleben F, Wittlieb J,
761 Klostermeier UC, Rosenstiel P, Oberg H-H, Domazet-Lošo T, Sugimoto T,
762 Niwa H & Bosch TCG (2012) Molecular Signatures of the Three Stem Cell
763 Lineages in Hydra and the Emergence of Stem Cell Function at the Base of
764 Multicellularity. *Mol. Biol. Evol.* **29:** 3267–3280
765 He Y-F, Li B-Z, Li Z, Liu P, Wang Y, Tang Q, Ding J, Jia Y, Chen Z, Li L, Sun Y, Li X,
766 Dai Q, Song C-X, Zhang K, He C & Xu G-L (2011) Tet-Mediated Formation of 5-
767 Carboxylcytosine and Its Excision by TDG in Mammalian DNA. *Science* **333:**
768 1303–1307
769 Ikegami K, Ohgane J, Tanaka S, Yagi S & Shiota K (2009) Interplay between DNA
770 methylation, histone modification and chromatin remodeling in stem cells
771 and during development. *Int. J. Dev. Biol.* **53:** 203–214
772 Ito S, Shen L, Dai Q, Wu SC, Collins LB, Swenberg JA, He C & Zhang Y (2011) Tet
773 Proteins Can Convert 5-Methylcytosine to 5-Formylcytosine and 5-
774 Carboxylcytosine. *Science* **333:** 1300–1303
775 De Juan D, Pazos F & Valencia A (2013) Emerging methods in protein co-
776 evolution. *Nat. Rev. Genet.* **14:** 249–261
777 Juan D, Rico D, Marques-Bonet T, Fernández-Capetillo O & Valencia A (2013)
778 Late-replicating CNVs as a source of new genes. *Biol. Open* **2:** 1402–1411
779 Kharchenko PV, Alekseyenko AA, Schwartz YB, Minoda A, Riddle NC, Ernst J, Sabo

780 PJ, Larschan E, Gorchakov AA, Gu T, Linder-Basso D, Plachetka A, Shanower
781 G, Tolstorukov MY, Luquette LJ, Xi R, Jung YL, Park RW, Bishop EP, Canfield
782 TK, et al (2011) Comprehensive analysis of the chromatin landscape in
783 Drosophila melanogaster. *Nature* **471:** 480–485
784 Li H & Durbin R (2009) Fast and accurate short read alignment with Burrows-
785 Wheeler transform. *Bioinformatics* **25:** 1754–1760
786 Liyanage VRB, Jarmasz JS, Murugeshan N, Del Bigio MR, Rastegar M & Davie JR
787 (2014) DNA Modifications: Function and Applications in Normal and Disease
788 States. *Biology* **3:** 670–723
789 Matarese F, Carrillo-de Santa Pau E & Stunnenberg HG (2011) 5-
790 Hydroxymethylcytosine: a new kid on the epigenetic block? *Mol. Syst. Biol.* **7:**
791 562–562
792 McLean CY, Bristor D, Hiller M, Clarke SL, Schaar BT, Lowe CB, Wenger AM &
793 Bejerano G (2010) GREAT improves functional interpretation of cis-
794 regulatory regions. *Nat. Biotechnol.* **28:** 495–501
795 Mitra K, Carvunis A-R, Ramesh SK & Ideker T (2013) Integrative approaches for
796 finding modular structure in biological networks. *Nat. Rev. Genet.* **14:** 719–
797 732
798 Moen EL, Mariani CJ, Zullow H, Jeff-Eke M, Litwin E, Nikitas JN & Godley LA
799 (2015) New themes in the biological functions of 5-methylcytosine and 5-
800 hydroxymethylcytosine. *Immunol. Rev.* **263:** 36–49
801 Nenadic O & Greenacre M (2007) Correspondence Analysis in R, with Two- and
802 Three-dimensional Graphics: The ca Package. *J. Stat. Softw.* **20:** 1–13
803 Papp B & Plath K (2012) Pluripotency re-centered around Esrrb. *EMBO J.* **31:**
804 4255–4257
805 Pastor WA, Pape UJ, Huang Y, Henderson HR, Lister R, Ko M, McLoughlin EM,
806 Brudno Y, Mahapatra S, Kapranov P, Tahiliani M, Daley GQ, Liu XS, Ecker JR,
807 Milos PM, Agarwal S & Rao A (2011) Genome-wide mapping of 5-
808 hydroxymethylcytosine in embryonic stem cells. *Nature* **473:** 394–397
809 Perner J, Lasserre J, Kinkley S, Vingron M & Chung H-R (2014) Inference of
810 interactions between chromatin modifiers and histone modifications: from
811 ChIP-Seq data to chromatin-signaling. *Nucleic Acids Res.* **42:** 13689–13695
812 Pfeifer GP, Kadam S & Jin S-G (2013) 5-hydroxymethylcytosine and its potential
813 roles in development and cancer. *Epigenetics Chromatin* **6:** 10
814 Powell S, Forslund K, Szklarczyk D, Trachana K, Roth A, Huerta-Cepas J, Gabaldón
815 T, Rattei T, Creevey C, Kuhn M, Jensen LJ, von Mering C & Bork P (2014)
816 eggNOG v4.0: nested orthology inference across 3686 organisms. *Nucleic*
817 *Acids Res.* **42:** D231–239
818 Raiber E-A, Beraldi D, Ficz G, Burgess HE, Branco MR, Murat P, Oxley D, Booth MJ,
819 Reik W & Balasubramanian S (2012) Genome-wide distribution of 5-
820 formylcytosine in embryonic stem cells is associated with transcription and
821 depends on thymine DNA glycosylase. *Genome Biol.* **13:** R69
822 Schreiber SL & Bernstein BE (2002) Signaling Network Model of Chromatin. *Cell*
823 **111:** 771–778
824 Scott-Phillips TC (2008) Defining biological communication. *J. Evol. Biol.* **21:**
825 387–395
826 Smith T late JM & Harper D (2003) Animal Signals Oxford Series in Ecology and
827 Evolution
828 Song C-X, Szulwach KE, Fu Y, Dai Q, Yi C, Li X, Li Y, Chen C-H, Zhang W, Jian X,

829 Wang J, Zhang L, Looney TJ, Zhang B, Godley LA, Hicks LM, Lahn BT, Jin P &
830 He C (2011) Selective chemical labeling reveals the genome-wide
831 distribution of 5-hydroxymethylcytosine. *Nat. Biotechnol.* **29:** 68–72
832 Stroud H, Feng S, Morey Kinney S, Pradhan S & Jacobsen SE (2011) 5-
833 Hydroxymethylcytosine is associated with enhancers and gene bodies in
834 human embryonic stem cells. *Genome Biol.* **12:** R54
835 Suzuki R & Shimodaira H (2006) Pvclust: an R package for assessing the
836 uncertainty in hierarchical clustering. *Bioinforma. Oxf. Engl.* **22:** 1540–1542
837 Szulwach KE, Li X, Li Y, Song C-X, Han JW, Kim S, Namburi S, Hermetz K, Kim JJ,
838 Rudd MK, Yoon Y-S, Ren B, He C & Jin P (2011) Integrating 5-
839 Hydroxymethylcytosine into the Epigenomic Landscape of Human
840 Embryonic Stem Cells. *PLoS Genet* **7:** e1002154
841 Vaissière T, Sawan C & Herceg Z (2008) Epigenetic interplay between histone
842 modifications and DNA methylation in gene silencing. *Mutat. Res.* **659:** 40–48
843 Vella P, Scelfo A, Jammula S, Chiacchiera F, Williams K, Cuomo A, Roberto A,
844 Christensen J, Bonaldi T, Helin K & Pasini D (2013) Tet Proteins Connect the
845 O-Linked N-acetylglucosamine Transferase Ogt to Chromatin in Embryonic
846 Stem Cells. *Mol. Cell* **49:** 645–656
847 Wang J, Hevi S, Kurash JK, Lei H, Gay F, Bajko J, Su H, Sun W, Chang H, Xu G,
848 Gaudet F, Li E & Chen T (2009) The lysine demethylase LSD1 (KDM1) is
849 required for maintenance of global DNA methylation. *Nat. Genet.* **41:** 125–
850 129
851 Wang J, Scully K, Zhu X, Cai L, Zhang J, Prefontaine GG, Krones A, Ohgi KA, Zhu P,
852 Garcia-Bassets I, Liu F, Taylor H, Lozach J, Jayes FL, Korach KS, Glass CK, Fu
853 X-D & Rosenfeld MG (2007) Opposing LSD1 complexes function in
854 developmental gene activation and repression programmes. *Nature* **446:**
855 882–887
856 Weigt M, White RA, Szurmant H, Hoch JA & Hwa T (2009) Identification of direct
857 residue contacts in protein-protein interaction by message passing. *Proc.*
858 *Natl. Acad. Sci. U. S. A.* **106:** 67–72
859 Williams K, Christensen J, Pedersen MT, Johansen JV, Cloos PAC, Rappsilber J &
860 Helin K (2011) TET1 and hydroxymethylcytosine in transcription and DNA
861 methylation fidelity. *Nature* **473:** 343–348
862 Wu H, D'Alessio AC, Ito S, Wang Z, Cui K, Zhao K, Sun YE & Zhang Y (2011)
863 Genome-wide analysis of 5-hydroxymethylcytosine distribution reveals its
864 dual function in transcriptional regulation in mouse embryonic stem cells.
865 *Genes Dev.* **25:** 679–684
866 Yang X, Ongusaha PP, Miles PD, Havstad JC, Zhang F, So WV, Kudlow JE, Michell
867 RH, Olefsky JM, Field SJ & Evans RM (2008) Phosphoinositide signalling links
868 O-GlcNAc transferase to insulin resistance. *Nature* **451:** 964–969
869 Ye T, Krebs AR, Choukrallah M-A, Keime C, Plewniak F, Davidson I & Tora L
870 (2011) seqMINER: an integrated ChIP-seq data interpretation platform.
871 *Nucleic Acids Res.* **39:** e35
872 Zhang Y, Wong C-H, Birnbaum RY, Li G, Favaro R, Ngan CY, Lim J, Tai E, Poh HM,
873 Wong E, Mulawadi FH, Sung W-K, Nicolis S, Ahituv N, Ruan Y & Wei C-L
874 (2013) Chromatin connectivity maps reveal dynamic promoter–enhancer
875 long-range associations. *Nature* **504:** 306–310
876 Zwaka TP (2012) Pluripotency network in embryonic stem cells: maybe Leibniz
877 was right all along. *Cell Stem Cell* **11:** 441–442

Figure legends

Figure 1. A framework to study communication among chromatin components

Our network approach is based on a classification of epigenomic features into three component classes, where histone and cytosine modifications are always considered to be signals and the chromatin-related proteins (CrPs) can be either co-occurring (or mutually exclusive) emitters (writers/erasers) or receivers (readers) of those epigenetic signals.

Figure 2. Chromatin communication network in ESCs

A full chromatin communication network in which the edges represent positive or negative interactions that indicate genomic co-localization or mutual exclusion, respectively. Arrows associated with the directional edges represent communication flux for emitter-signal or signal-receiver pairs retrieved from the literature. The colors indicate membership of known protein complexes. B Emitters and receivers of the H3K79me2 hub signal. C Emitters and receivers of the 5hmC hub signal.

Figure 3. Co-evolution of CrPs

Coupling analysis of the phylogenetic histories of CrPs revealed significant co-evolution between emitters and receivers of 5hmC and 5fC. Co-evolving pairs are indicated by thick colored dashed lines. The grey lines indicate co-localization or mutual exclusion in the chromatin communication network (see Figure 2 for more details).

Figure 4. Chromnets recover known protein complexes and star-shaped structures

The chromnets are sub-networks of interactions with similar co-occurrence across the chromatin states and they have different topologies. Each bar plot indicates the overall enrichment of the chromatin states in each chromnet along (see B for details of the chromatin states). B Star-like 5hmC sub-network and the overall enrichment of chromatin states.

910 **Figure 5. 5hmC genomic regions have different functional enrichment depending**
911 **on the co-localizing partner**
912 A-D Read densities over a 10Kb windows centered on the 5hmC-ESRRB (A),
913 5hmC-LSD1 (B), 5hmC-TET1 (C) and 5hmC-OGT (D) peaks. We calculated the
914 read density of 5hmC, ESRRB, LSD1, TET1 (N- and C-terminal ChIP-seqs) and
915 OGT in 10Kb windows centered on the genomic bins (200 bp), where 5hmC co-
916 localizes exclusively with each specific partner (i.e.: the rest of the 5hmC
917 interactors are not present). The read density plots were obtained with the
918 SeqMINER platform v1.3.3e (Ye *et al*, 2011). The average density of the reads in
919 50 bp bins was plotted from the center of the 5hmC independent genomic regions
920 to +/-5000 bp. E Gene Ontology enrichment analysis of peaks in A-D using
921 GREAT.

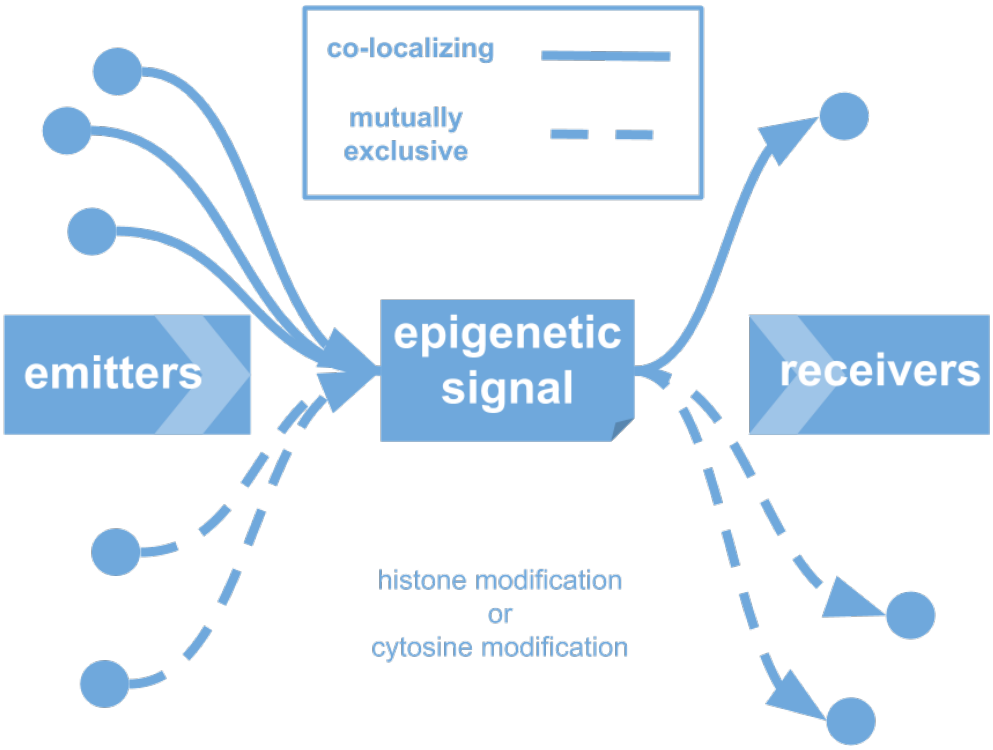
co-localizing
mutually exclusive
emitters
epigenetic signal
receivers
histone modification
or
cytosine modification

Figure 1

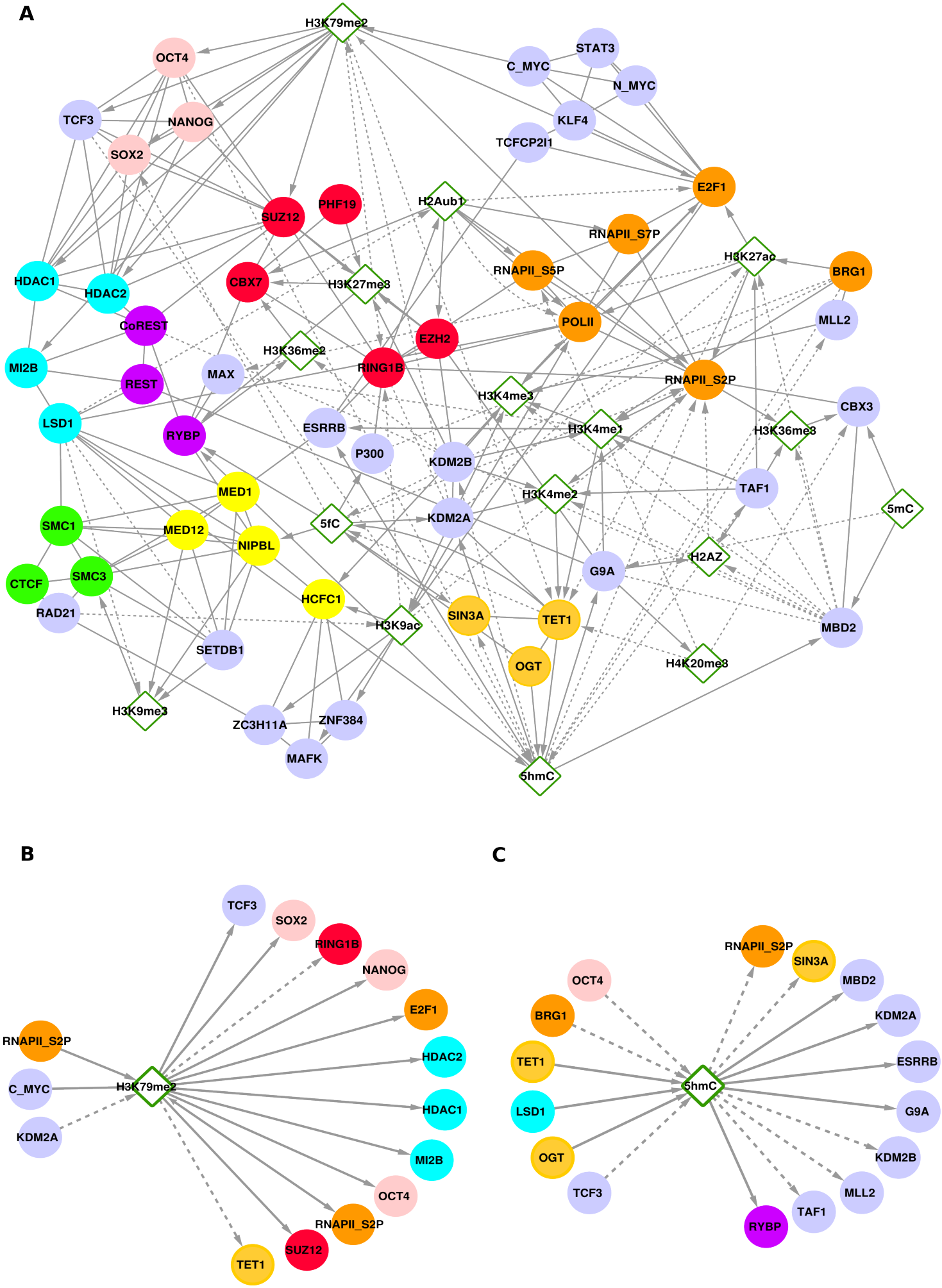
A
H3K79me2
OCT4
STAT3
C_MYC
N_MYC
TCF3
NANOG
KLF4
SOX2
TCFCP2I1
E2F1
PHF19
H2Aub1
SUZ12
RNAPII_S7P
H3K27ac
BRG1
HDAC1
HDAC2
CBX7
H3K27me3
RNAPII_S5P
CoREST
POLII
MLL2
EZH2
H3K36me2
MI2B
MAX
RING1B
REST
RNAPII_S2P
H3K4me3
CBX3
LSD1
RYBP
ESRRB
H3K4me1
H3K36me3
P300
KDM2B
MED1
H3K4me2
TAF1
5mC
SMC1
MED12
5fC
KDM2A
NIPBL
H2AZ
G9A
CTCF
SMC3
HCFC1
RAD21
SIN3A
TET1
H3K9ac
MBD2
SETDB1
OGT
H4K20me3
H3K9me3
ZC3H11A
ZNF384
MAFK
5hmC
B
TCF3
SOX2
RING1B
NANOG
E2F1
RNAPII_S2P
HDAC2
C_MYC
H3K79me2
HDAC1
KDM2A
MI2B
OCT4
RNAPII_S2P
SUZ12
TET1
C
RNAPII_S2P
SIN3A
OCT4
MBD2
BRG1
KDM2A
TET1
ESRRB
5hmC
LSD1
G9A
OGT
KDM2B
TCF3
MLL2
TAF1
RYBP

Figure 2

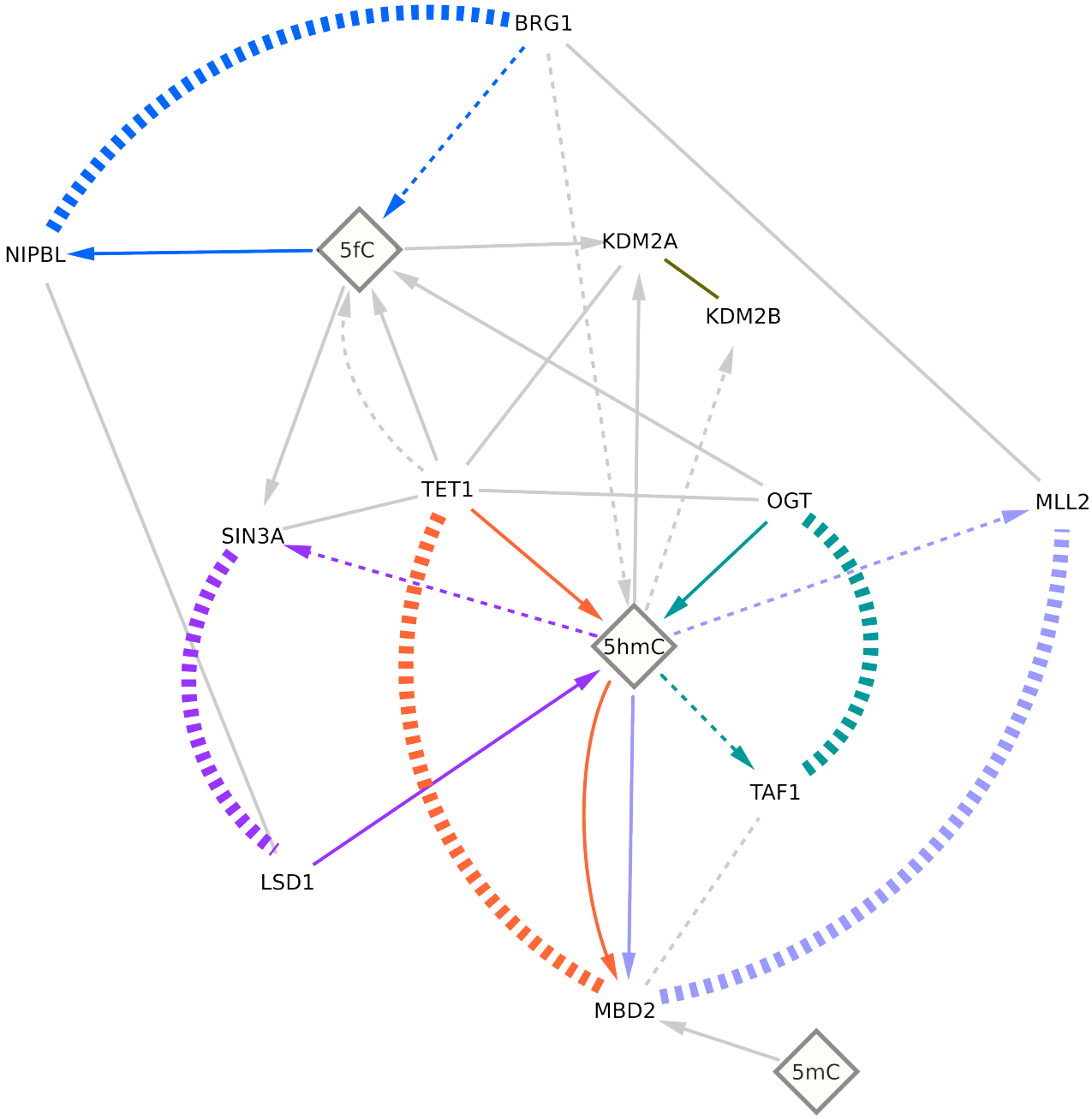
BRG1
NIPBL
5fC
KDM2A
KDM2B
TET1
OGT
MLL2
SIN3A
5hmC
TAF1
LSD1
MBD2
5mC

Figure 3

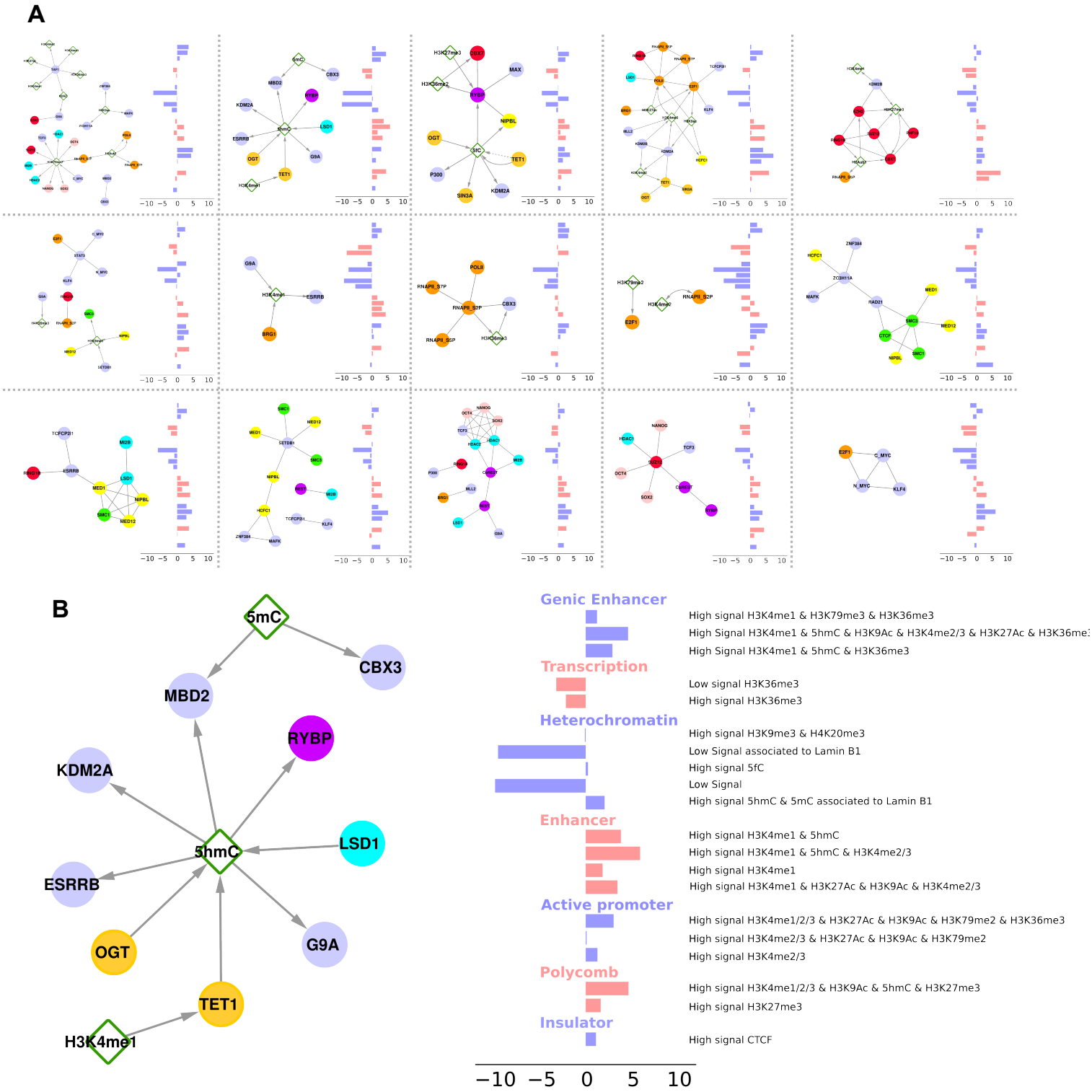
A
B
5mC
CBX3
MBD2
RYBP
KDM2A
5hmC
LSD1
ESRRB
OGT
G9A
TET1
H3K4me1
Genic Enhancer
High signal H3K4me1 & H3K79me3 & H3K36me3
High Signal H3K4me1 & 5hmC & H3K9Ac & H3K4me2/3 & H3K27Ac & H3K36me3
High Signal H3K4me1 & 5hmC & H3K36me3
Transcription
Low signal H3K36me3
High signal H3K36me3
Heterochromatin
High signal H3K9me3 & H4K20me3
Low Signal associated to Lamin B1
High signal 5fC
Low Signal
High signal 5hmC & 5mC associated to Lamin B1
Enhancer
High signal H3K4me1 & 5hmC
High signal H3K4me1 & 5hmC & H3K4me2/3
High signal H3K4me1
High signal H3K4me1 & H3K27Ac & H3K9Ac & H3K4me2/3
Active promoter
High signal H3K4me1/2/3 & H3K27Ac & H3K9Ac & H3K79me2 & H3K36me3
High signal H3K4me2/3 & H3K27Ac & H3K9Ac & H3K79me2
High signal H3K4me2/3
Polycomb
High signal H3K4me1/2/3 & H3K9Ac & 5hmC & H3K27me3
High signal H3K27me3
Insulator
High signal CTCF
−10 −5 0 5 10

Figure 4

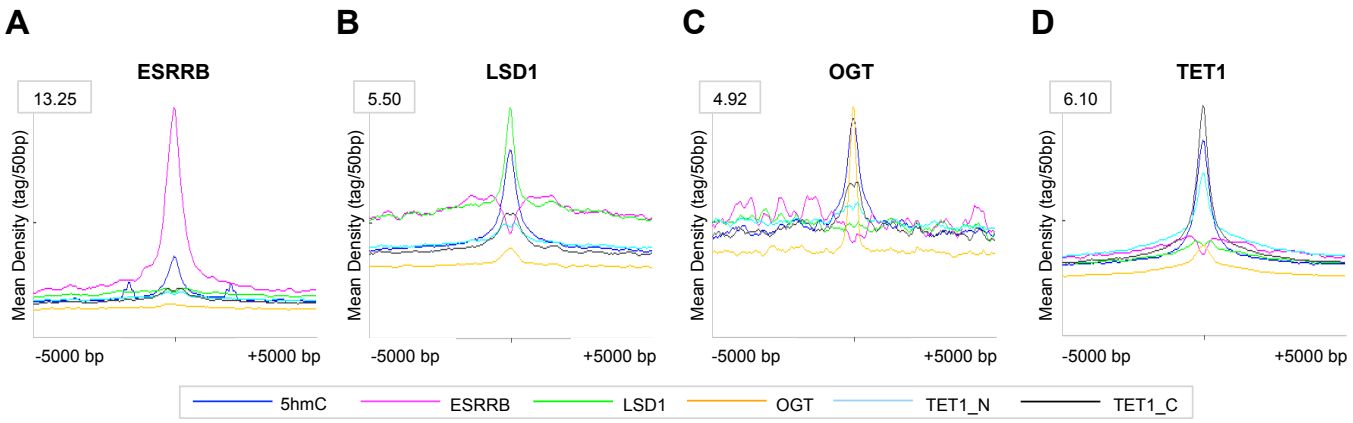

E

GO term	ESRRB	LSD1	TET1	OGT
Maturation of SSU-rRNA	■			
Regative regulation of MAPK cascade	■			
Plasma membrane organization	■			
Intrinsic apoptotic signaling pathway	■			
Cell-cell junction organization	■			
Epithelial cell morphogenesis	■			
Somatic stem cell maintenance	■		■	
Regulation of Notch signaling pathway	■		■	
Mesoderm morphogenesis	■		■	
Histone acetylation	■	■		
Regulation of gene expression, epigenetic	■	■		
DNA methylation or demethylation		■		
Histone H3-H4 acetylation		■		
Placenta development		■		
Blastocyst formation		■		
Proteasomal protein catabolic process		■		
Regulation of translation		■		
Regulation of stem cell maintenance			■	
Regulation of TGF-beta receptor signaling			■	
Apoptotic process involved in morphogenesis			■	
Cell-cell signaling involved in cell fate commitment			■	
Developmental induction			■	
Mesoderm development			■	
Body and head morphogenesis			■	■
Carbohydrate biosynthetic process				■
Glycerophospholipid metabolic process				■
Regulation of lipid storage				■
Maintenance of location in cell				■
Modulation by virus of host morphology or physiology				■
Regulation of organelle organization				■
Regulation of chromatin organization				■
Regulation of histone modification				■
Regulation of cytokinesis				■

Figure 5